Karaelmas Science and Engineering Journal
Journal home page: http://fbd.beun.edu.tr
DOI: 10.7212/zkufbd.v9i1.1180

Research Article
Received / Geliş tarihi : 26.10.2017
Accepted / Kabul tarihi : 27.01.2018

Spectral and Theoretical Analysis of *N*-[4-(3-methyl-3-phenyl-cyclobutyl)-thiazol-2-yl]-*N´*-thiophen-2ylmethylene-Chloro-acetic Acid Hydrazide by DFT Method

N-[4-(3-metil-3-fenil-siklobutil)-tiazol-2-yl]-N´-tiyofen-2ylmetilene-Khloro-Asetik Asit Hidrazid'in DFT Metodu Kullanılarak Spektral ve Teorik Analizi

Sibel Demir Kanmazalp[1*], Muharrem Dinçer[2], Alaaddin Çukurovalı[3], İbrahim Yılmaz[4]

[1] Gaziantep University, Technical Science Vocational School, Gaziantep, Turkey
[2] Ondokuz Mayıs University, Faculty of Arts and Sciences, Department of Physics, Samsun, Turkey
[3]Firat University, Faculty of Science, Department of Chemistry, Elaziğ, Turkey
[4]Karamanoğlu Mehmet Bey University, Faculty of Science, Department of Chemistry, Karaman, Turkey

Abstract

This study presents a combined experimental and theoretical research on an *N*-[4-(3-methyl-3-phenyl-cyclobutyl)-thiazol-2-yl]-*N´*-thiophen-2ylmethylene-Chloro-acetic acid hydrazide compound. The optimized molecular structure, ^{1}H and ^{13}C chemical shift values and vibrational assignments of the titled compound were examined by depending on the density functional method and by using 6-31G(d), 6-31G(d,p) and 6-311G(d,p) basis sets. Moreover, HOMO–LUMO analysis and molecular electrostatic potential were carried out in order explore charge delocalization on this molecule.

Keywords: Frontier molecular orbitals, Molecular electrostatic potential, IR and NMR spectroscopy, X-ray structure determination

Öz

Bu çalışma *N*-[4-(3-metil-3-fenil-siklobutil)-tiazol-2-yl]-*N´*-tiyofen-2ylmetilene-Khloro-asetik asit hidrazid bileşiğinin deneysel ve teorik çalışmasını gösterir. Optimize edilmiş moleküler yapı, ^{1}H ve ^{13}C kimyasal kayma değerleri ve titreşim frekansları DFT metodu ile birlikte 6-31G(d), 6-31G(d,p) ve 6-311G(d,p) baz setleri kullanılarak incelenmiştir. İlaveten molekülдeki yük delokalizasyonu incelemek için HOMO-LUMO analizi ve moleküler elektrostatik potansiyeli araştırılmıştır.

Anahtar Kelimeler: Sınır moleküler orbitaller, Moleküler elektrostatik potansiyel, IR ve NMR spektroskopisi, X-ışını yapı tanımı

1. Introduction

The chemistry of aminothiazoles and their derivatives has attracted the attention of chemists, because they exhibit an important biological activity in medicinal chemistry Pozharskii et al. 1997, Wipf and Wang 2007 such as antibiotic, anti-inflammatory, antihelmintic, or fungicidal properties (Metzger 1979, Koike et al. 1999, Walczynski et al. 1999). 2-Aminothiazoles are mainly known as biologically active compounds with a broad range of activities and as intermediates in the synthesis of antibiotics, well-known sulfa drugs, and some dyes (Patt et al. 1992, Sharma et al. 1998). In addition, it has been proved that 3-substituted cyclobutane carboxylic acid derivatives exhibit anti-inflammatory and antidepressant activities Jaen et al. 1990 and also liquid crystal properties (Tsuji et al. 1994).

In this study, we present the results of a detailed investigation of the synthesis and structural characterization of a *N*-[4-(3-methyl-3-phenyl-cyclobutyl)-thiazol-2-yl]-*N´*-thiophen-2ylmethylene-Chloro-acetic acid hydrazide (NNT2CAH) compound by using single crystal X-ray diffraction, IR and NMR spectroscopy and quantum chemical methods. The geometrical parameters, fundamental frequencies and GIAO ^{1}H and ^{13}C NMR chemical shift values of the title compound in the ground state have been calculated by using the B3LYP method. A comparison of the experimental and theoretical spectra can be very useful in making correct assignments and understanding the basic chemical shift-

*Corresponding author: sibeld@gantep.edu.tr

Sibel Demir Kanmazalp orcid.org/0000-0002-5896-0966
Muharrem Dinçer orcid.org/0000-0003-3960-9991
Alaaddin Çukurovalı orcid.org/0000-0002-8297-2350
İbrahim Yılmaz orcid.org/0000-0002-9447-3065

molecular structure relationship. Furthermore, the molecular electrostatic potential, and frontier molecular orbitals, were studied at the B3LYP/6-311G(d, p) level.

2. Materials and Method

2.1 Crystallographic Analysis

Single crystal X-ray data were collected on an STOE diffractometer with an IPDS(II) image plate detector (Mo K_α radiation) at 296 K. The crystal was solved by direct methods by using SHELXS-97 and refinement was carried out with full-matrix least-squares methods based on F^2 with the SHELXL-97 software package (Sheldrick 1997). All hydrogen atoms were refined in isotropic approximation in a riding model with the $U_{iso}(H)$ parameters which equal to 1.2 $U_{eq}(C_i)$, for methyl groups which equal to 1.5 $U_{eq}(C_{ii})$, where $U(C_i)$ and $U(C_{ii})$ are, respectively the equivalent thermal parameters of the carbon atoms to which corresponding H atoms are bonded. The crystal data and experimental parameters are given in Table 1.

Table 1. Crystallographic data for NNT2CAH

Formula	$C_{21}H_{20}ClN_3OS_2$
CCDC	775739
Formula Weight	430
Temperature[K]	296
Wavelength [Å]	0.71073
Crystal system	Orthorhombic
Space group	$P\ 2_12_12_1$
a [Å]	5.9330 (3)
b [Å]	17.2192(12)
c [Å]	20.2868(12)
α [°]	90
β [°]	90
γ [°]	90
V[Å^3]	2072.53(2)
Z	4
D_{calc} [g/cm^3]	1.38
F(000)	895.9
h, k, l Range	-7≤h≤7 -21≤k≤21 -17≤l≤25
Reflections collected	11938
Independent reflections	4357
R_{int}	0.053
Reflections observed [I≥2σ(I)]	2649
R [I>2σ(I)]	0.046
*R*w [I>2σ(I)]	0.0691
Goodness-of-fit on Indicator	0.891
Structure determination	Shelxs-97
Refinement	Full matrix
$(\Delta\sigma)_{max}$, $(\Delta\sigma_{min})$ [e/ Å^3]	0.16, -0.16

2.2. Instrumentation

FT-IR spectra were measured by ATI Unicam-Mattson 1000 FT-IR spectrometer in the frequency range of 4000–400 cm^{-1} by using KBr disc. The FT-IR spectra were recorded at room temperature at the spectral resolution of 1 cm^{-1}. ^{1}H and ^{13}C NMR spectra were recorded with Bruker Avance III 400 MHz spectrometer. Chemical shifts were reported on a scale which correlate with TMS.

2.3. Synthesis

The synthesis of the title compound was carried out in the following reaction Scheme. A solution of 0.3535 gram (1 mmol) of *N*-thiophen-2-ylmethylene-*N´*-[4-(3-methyl-3-phenyl-cyclobutyl)-thiazol-2-yl]-hydrazine was dissolved in 20 mL of dioxane containing 1 mmol triethylamine. To this solution, 90 µL (1 mmol) of chloroacetyl chloride solution in 20 mL 1,4-dioxane was added dropwise in a two hour period at room temperature by stirring. The mixture was stirred for another two hours, then was neutralized with 5% aqueous ammonia (if necessary, but generally it is necessary). Thus, the precipitated compound was filtered, washed with copious water and crystallized from ethanol. The reaction sequence of synthesis of the title compound is shown in Scheme.

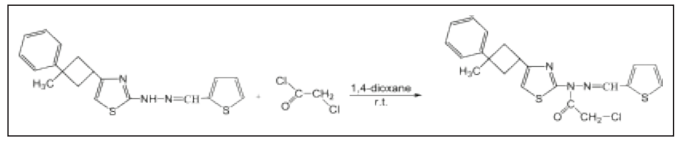

Scheme. Reaction sequence of synthesis of NNT2CAH.

2.4. Computational details

Initial geometry generated from standard geometrical parameters was minimized. The optimized structural parameters were used in the vibrational frequency calculations at the DFT level to characterize all the stationary points as minima. The calculated NMR, molecular electrostatic potential and frontier orbitals were calculated using the same method and then vibrational frequencies of normal modes scaled 0.9613 for 6-31G(d) (Foresman et al. 1996, Merrick et al. 2007) 0.9611 for 6-31G(d,p) (Schlegel 1982, Hehre et al. 1972) and 0.9670 6-311G(d, p) (Andersson et al. 2005) with B3LYP. Additionally, we calculated the ^{1}H and ^{13}C NMR chemical shifts for this structure using

GIAO model at the same level. These calculations were performed at DFT (B3LYP) method using the Gaussian 03W program package (Frisch et al. 2003).

3. Results

3.1 Description of The Crystal Structure

The molecular structure of the title compound is shown in Figure 1(A). Thermal ellipsoids are drawn at 40% probability level. The crystal data and experimental parameters are given in Table 1. Besides, hydrogen bonding geometry is given in Table 2.

In the asymmetry unit, the thiazole ring and acetic acid hydrazide group are coplanar. The thiazole ring makes the dihedral angle with the acetic acid hydrazide group of 11.96(0.22). There is a significant intramolecular C15–H15…N1 hydrogen bonds forming the corresponding pseudo five-membered ring. The crystal packing diagram of NNT2CAH is shown in Figure 1(B). The molecular conformation was stabilized by intra and inter molecular C—H…N/O/Cl and C—H…π (C4…B ring 3.772(3) Å) hydrogen bonds (Figure 1(B) and Table 2). The short C20–C21 distance [1.508(4) Å] may be due to a collective interaction of C21 with the nearby hydrazide group and O1 atom, an intramolecular close contact interaction with the nearby nitrogen atom in thiazole (C15–H15…N1; see Table 2), and an C2–H2…O1 intermolecular interaction (H2…O1= 2.86 Å; symmetry code: -1/2+x, 1/2-y, 1-z; that may influence the bond strength of the C20–C21. Other hydrogen bonds are listed in Table 2. The hydrazide group lies in a trans configuration along the N(3)–C(15) bond (torsion angles C15–N3–N2–C21= 169.3(3)° and C15–N3–N2–C1= -14.4(4)°, respectively).

3.2 Optimized Molecular Geometry

Listed in Table 3 are, the optimized geometrical parameters of NNT2CAH, calculated at B3LYP/6-31G(d)/6-31G(d,p)/6-311G(d,p) basis sets in the gas phase which are in accordance with the atom numbering scheme are given in Figure 1(A). These indicate a slight underestimate or overestimate of some bond lengths, as a result, 6-31G(d,p) basis set predicts bond lengths in an excellent agreement

Table 2. Hydrogen bonding geometry [Å, °] for the NNT2CAH.

D—H···A [Å]	D—H [Å]	H···A [Å]	D···A [Å]	D—H···A [°]
C15—H15…N1	0.93	2.11	2.776(4)	126
C18—H18…^{O}1i	0.93	2.92	3.813	162
C13—H13…Cl1^{ii}	0.93	3.04	3.741	134
C2—H2…O1^{iii}	0.93	2.86	3.53	130
C4—H4…π	0.98	2.79	3.772	179

i:5/2-x,-y,-1/2+z, ii: 3/2-x, -y, -1/2+z iii: -1/2+x,1/2-y,1-z

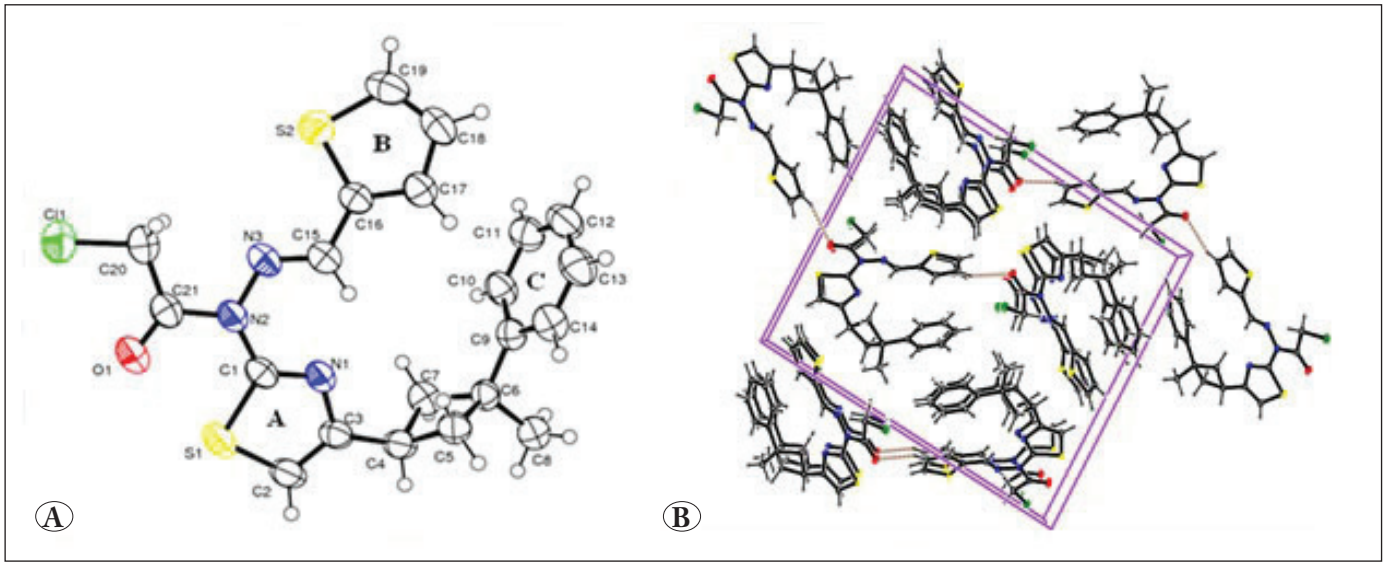

Figure 1. (A) Molecular structure with atomic numbering for NNT2CAH **(B)** Packing diagram of NNT2CAH.

with X-ray data. However, for the bond angles of 6-31G(d) basis set are better when compared with experimental results. We present correlation graphics in Figure 2 based on these calculations. Considering the comparison above, although the theoretical and experimental values slightly differentiate from each other the optimized structural parameters can reproduce the experimental one well and they are the basis for following discussion.

A logical method for globally comparing of the structures obtained with the theoretical calculations is to superimpose the molecular skeleton with that obtained from X-ray diffraction, giving an RMSE of 0.366 Å for 6–31G(d), 0.362 Å for 6–31G(d,p) and 0.383 Å for 6–311G(d,p) calculated by using B3LYP method (Figure 3). Consequently, the 6–31G(d,p) basis set correlates well with the geometrical parameters when compared with other basis sets. Figure 3 represents atom-by-atom superimposition of the structures were calculated (black) in the X-ray structure (red) of the title compound.

3.3. Vibrational Analysis

Assignment of organic systems can be proposed on the basis of frequency agreement between the computed harmonics and the observed fundamental modes. The resulting vibrational wave numbers for the optimized geometry and the proposed assignments are given in Table 4. Based on the results of the normal coordinate calculations the vibrational spectral data obtained from the solid phase FT-IR spectra are assigned. All vibrational calculations were performed in the harmonic approximation.

In the heteroaromatic compounds, the C–H stretching vibrations normally occur at 3100–3000 cm^{-1} (Stuart 2008). These vibrations were not found to be the influence to the nature and the position of the substituent and they typically exhibit weak bands when compared with the aliphatic stretching vibrations. In infrared spectra, most of the aromatic compounds have nearly four peaks in the region 3080–3010 cm^{-1} due to the ring C–H stretching bands. IR frequencies of C–H band are a function of sp hybridization (Pavia et al. 2001). Four IR bands were observed at 3115, 3104, 3080 and 2925 cm^{-1} were assigned to the C–H stretching vibration for NNT2CAH. The second band belongs to the symmetric and the third to the asymmetric stretching band. In the higher frequency region, almost all of the vibrations belong to CH_3 and CH_2 stretching vibrations.

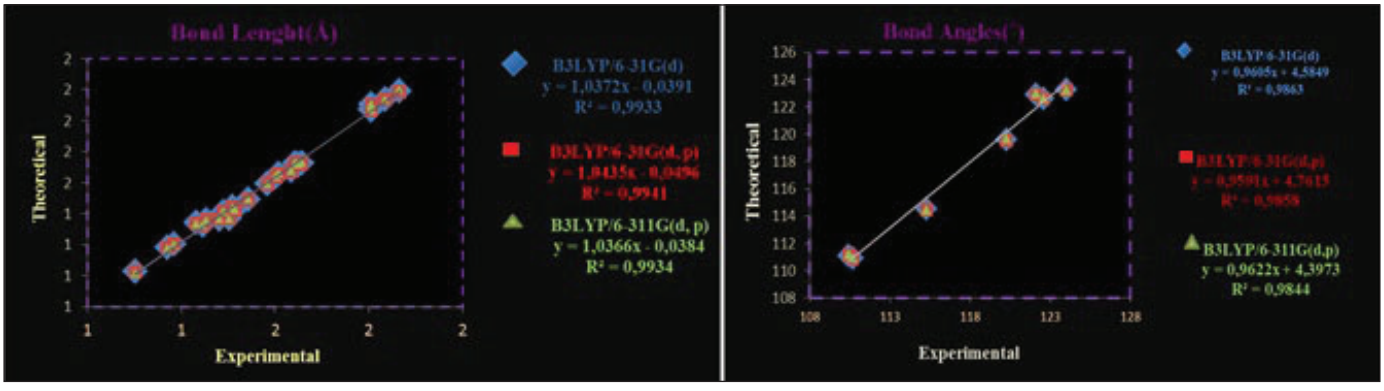

Figure 2. Correlation graphics of calculated and experimental geometric parameters of NNT2CAH.

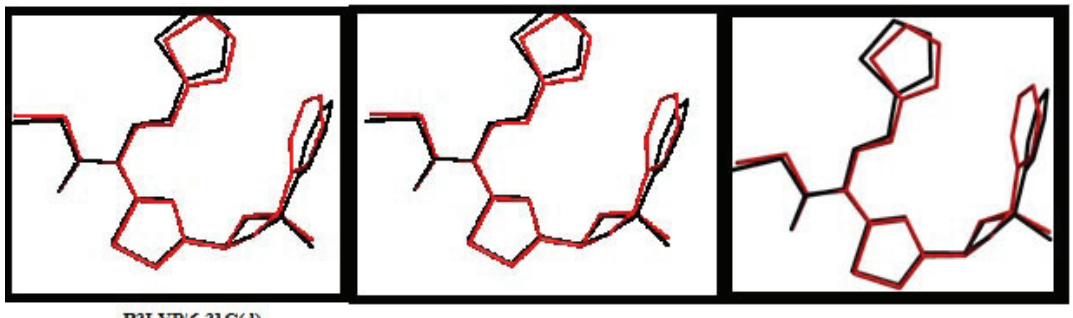

Figure 3. Atom-by-atom superimposition of the structures calculated (black) as (B3LYP/6–31G(d), 6–31G(d,p) and as 6–311G(d,p)) on the X-ray structure (red) of NNT2CAH hydrogen atoms have been omitted for clarity.

If a CH_3 group presents in a compound, it can give rise to one asymmetric and one symmetric stretching vibration. In this molecule, these vibrations were observed at 2959 and 2563 cm^{-1}, respectively. The range of frequencies obtained by B3LYP method in this region are 2987/2921 cm^{-1} for 6-31G(d) and 2986/2916 cm^{-1} for 6-31G(d,p) 2982/2919 cm^{-1} for 6-311G(d,p) basis sets, respectively. CH_2 stretching vibration modes are observed at 3036, 3021, 2975 and 2862 cm^{-1}. The first of these modes is the asymmetric vibration of the cyclobutane ring and chloro-asetic acid group and the others are a symmetric vibrations of same groups, respectively. Belonging to CH_2 other calculated vibrations can also be seen in Table 4. Generally, the C=C stretching vibrations in aromatic compounds compose six bands in the region of 1650–1430 cm^{-1}. These bands show the intention to shift to the lower wavenumber with heavy substituents and an increase in a number of substituents on the compound gives rise to these vibrations, and were observed in the wide region of FT-IR spectrum (Roeges 1994). The characteristic band of C=C stretching vibration of the

Table 3. Selected optimized and experimental geometries parameters of NNT2CAH.

Parameters	Experimental		DFT/B3LYP	
		6-31G(d)	6-31G(d,p)	6-311G(d,p)
Bond lengths[Å]				
C21-O1	1.202 (4)	1.214	1.214	1.207
C21-N2	1.391 (4)	1.405	1.405	1.407
C21-C20	1.508 (4)	1.530	1.529	1.528
C20-Cl1	1.766 (3)	1.795	1.794	1.797
S1-C2	1.705 (3)	1.739	1.739	1.737
S1-C1	1.735 (3)	1.768	1.768	1.767
N1-C1	1.284 (3)	1.303	1.303	1.300
N1-C3	1.382 (3)	1.382	1.382	1.381
C2-C3	1.347 (4)	1.363	1.363	1.361
S2-C19	1.706 (3)	1.733	1.733	1.731
S2-C16	1.706 (3)	1.752	1.751	1.750
N3-C15	1.271 (4)	1.290	1.290	1.286
N3-N2	1.403 (3)	1.384	1.384	1.382
N2-C1	1.415 (3)	1.410	1.410	1.411
C3-C4	1.483 (4)	1.496	1.496	1.495
Bond Angles[°]				
N3-C15-C16	120.3 (3)	119.594	119.553	119.656
C17-C16-S2	110.7 (2)	110.919	110.919	110.926
C15-C16-S2	124.0 (2)	123.261	123.282	123.224
N1-C1-N2	122.1 (3)	122.895	122.877	122.966
N1-C1-S1	115.3 (2)	114.510	114.496	114.400
N2-C1-S1	122.6 (2)	122.595	122.627	122.634
C21-C20-Cl1	110.4 (2)	111.120	111.177	111.161
Torsion angles[°]				
O1-C21-N2-N3	–174.8 (3)	179.997	179.995	179.985
C20-C21-N2-N3	5.4 (3)	-0.003	-0.006	-0.014
O1-C21-N2-C1	8.8 (4)	-0.001	-0.003	-0.008
C20-C21-N2-C1	–171.0 (2)	179.999	179.996	179.994
C15-N3-N2-C21	169.3 (3)	179.997	179.998	-179.993
N2-C21-C20-Cl1	175.1 (2)	-179.999	0.002	-179.994
N1-C3-C2-S1	1.2 (3)	-0.001	-179.998	-0.003

Table 4. Comparison of the observed and calculated vibrational spectra of NNT2CAH.

Assignments	Experimental	DFT/B3LYP		
	[cm^{-1}]	6-31G(d)	6-31G(d,p)	6-311G(d,p)
ν C-H (A)	3115	3139	3136	3135
ν_s C-H(C)	3104	3082	3079	3083
ν_{as} C-H(C)	3080	3065/3053	3062/3049	3072/3065
ν_{as} X–H_2(Δ)	3036	3011/3007	3010	3052/3011
ν_{as} C-H_2(E)	3021	3062	3056	3063
ν_s C- H_2(E)	2975	3009	3002	3011/2951
ν_{as} C-H_3	2959	2987	2986	2982
ν C-H (D)	2925	2965	2964	2969
ν_s C-H_2(D)	2862	2952-2949	2947	2951
ν_s C-H_3	2563	2921	2916	2919
ν C=O	1709	1728	1728	1726
ν C_{15}-N_3	1637	1598	1596	1593
ν C=C (C)	1594	1597/1573	1594-1570	1590
ν C-C (A+B)	1578	1526-1525	1525-1523	1521
γ C-H (C)	1476	1485	1478	1427
ν C=N (A)	1600	1474/1299/1313	1473/1294/1309	1466
ν C-C (B)	1429	1431	1429	1423
α C-H_2 (E)	1399	1412	1395	1453/1446
ω C-H_3	1374	1381	1367	1364
γ C-H (B+F)	1348	1366/1322	1361/1315	1363
ω C-H_2 (E)	1326	1290	1282	1282
ν C_6-C_9	1302	1281	1276	1276
ν C_{15}-C_{16}+ ν C_1-N_2-N_3	1240	1227	1225	1222
γ C-H(B)+ωC-H_2(E) + νC_1—N_1	1215	1222/1201	1216	1217
ν C_{21}-N_2-C_1+ α C-H(C)	1199	1171	1167	1196/1166
δ C-H_2(E)	1150	1153	1074	1149
Θ (A)	894	875	873	1007
Θ (C)	-	978	975	984
δ C-H (C)	950	954/930/890	957-936/890	950
δ C-H (B)	919	883	886	892
β (B)	856	835/740	834	838
ν C-S (A)	843	819	817	819
ν C-Cl	796	771	769	771
ω (C)	755	750/691	751/750	756
ν C-S (B)	736	740	739	744
ω C-H (B)	699	692	691	691
β deformation (C)	-	609	608	694
Θ (B)	617	659	658	569

Vibrational modes: ν, stretching; **s,** symmetric; **as,** asymmetric; α, scissoring; γ, rocking; ω, wagging; δ, twisting; θ, ring breathing; β, in-plane bending.
Abbreviations: A, thiazole ring; **B,** furan ring; **C,** phenyl ring; **D,** cyclobutane ring; **E,** chloro acetic acid group; **F,** hydrazide group.

phenyl ring of NNT2CAH appears at 1594 cm^{-1}. Stretching vibration of C=O group is expected to appear at 1715–1680 cm^{-1} (Roeges 1994). The very strong C=O experimental bands which were observed at 1709 cm^{-1} for NNT2CAH correspond to the stretching vibration of C=O group of chloro-acetic acid, which lie in a higher frequency region in the present case indicating the weak delocalization of a lone pair of electrons. The increase in conjugation, generally, leads to the intensification of infrared bands. The conjugation and the influence of intermolecular hydrogen bonding result in the lowering of the stretching wavenumbers of C=O vibration (Sıdır et al., 2010). Frequencies of C=O stretching for a DFT method vibrations are in good agreement with the experimental results.

Any deviation of the calculated wavenumber for this mode can be attributed to π-electron delocalization due to the conjugation or formation of hydrogen bonds (Panicker et al.2007). The identification of C–N vibrations is a very challenging task since the mixing of several bands could be possible in this region. However, with the help of theoretical calculations and percentage relative weight of vibrations the C–N stretching vibrations are identified and assigned in this study. The C–N stretching vibrations are assigned in the region 1382–1266 cm^{-1} for aromatic amines (Silverstein 2003). The C–N stretching modes appear at 1637, 1600, 1240 and 1199 cm^{-1} for NNT2CAH in the solid-state FT-IR spectra. The FT-IR band observed at 1637 cm^{-1} is the most intensive band in this region. For B3LYP level, calculated wavenumbers of these bands show excellent agreement with corresponding experimental ones for NNT2CAH. These results are detailed in Table 4. Here, it is important to conclude the vibrations of C-halogen bonds in the aromatic ring, because, the mixture of vibrational modes are possible due to a lack of symmetry and the presence of heavy atoms such as F, Cl, Br, I and S in the molecule (Yadav and Sing 1985). The C–S and S–H bonds are highly polarizable and hence produce stronger spectral activity. The C–S stretching vibration is expected in the region 710–685cm^{-1} (Coates 2000). The C–S stretching vibrations were observed at 843 and 736 cm^{-1} for NNT2CAH. The infrared band appearing at 796 cm^{-1} was designated to C–Cl stretching mode in this molecule. This C–Cl vibrational mode was reported at 795 cm^{-1} for N'-benzylidene-N-[4-(3-methyl-3-phenyl-cyclobutyl)-thiazol-2-yl]-Chloro-acetic acid hydrazide (Demir et al. 2012). On the other hand, C–S stretching in thiazole (ring A) and C–Cl stretching bands were calculated 819 and 771 cm^{-1} with B3LYP/6-31G(d) and B3LYP/6-311G(d,p), 817 and 769 cm^{-1} with B3LYP/6-31G(d,p), respectively.

3.4. Nuclear Magnetic Resonance

Since NMR chemical shifts bear witness to the electron density which is close to nuclei, the use of core pseudopotentials is in principle precluded. For this reason, these chemical shifts have been calculated with the GIAO (Gauge Invariant Atomic Orbitals) method (Wolinski et al. 1990) and these results relative to the TMS value are given in Table 5. The NNT2CAH compound has 21 different carbon atoms, which is consistent with the structure based on molecular symmetry. Calculated ^{1}H and ^{13}C isotropic chemical shielding values for TMS at the B3LYP level were obtained 32.10 ppm and 189.40 ppm for 6-31G(d) and 32.37 ppm and 193.97 ppm for 6-31G(d, p), and 31.99 ppm and 185.06 ppm for 6-311G(d, p) basis sets, respectively. The experimental values for ^{1}H and ^{13}C isotropic chemical shifts for TMS were 30.84 ppm and 188.1 ppm, respectively. Since experimental ^{1}H chemical shift values were not available for an individual hydrogen, we have presented the average values for aromatic CH_2 and CH_3 hydrogen atoms. In our present study the methyl protons at C8 appears as a singlet with three protons integral at 1.60 ppm. The singlet observed at 6.85 ppm was assigned to H2(C2) atoms that were calculated at 2.92 ppm (6-31G(d)) and 4 ppm (6-31G(d,p)) and 6.93 ppm (6- 311G(d,p)) for the B3LYP level. The CH_2 signals of the cyclobutane were observed at 2.52–2.68 ppm. Another CH_2 signal, C20(H20) in the chloro-acetic acid was observed at 4.82 ppm. Due to deshielding by the electronegative property of N1, N2, and S1 atoms, the chemical shift value of C1 which has a larger value than the others, was observed at 167.29 ppm. Besides, due to the shielding effect of the non-electronegative property of the hydrogen atom, the chemical shift value of C8 atom is lower than the others carbon peak (Karakurt et al. 2011). As shown in Table 5, theoretical ^{1}H and ^{13}C chemical shift results of the title compound were generally closer to the experimental ^{1}H and ^{13}C shift data.

3.5. Molecular Electrostatic Potential

The molecular electrostatic potential (MEP) is widely used as a reactivity map displaying most probable regions for the electrophilic attack of charged point-like reagents on organic molecules (Politzer 1981). The MEP of NNT2CAH is obtained based on the B3LYP/6-11G(d,p) optimized result and shown in Figure 4. The calculated 3D MEP contour map (red is negative, blue is positive) shows that the negative

Table 5. Theoretical and experimental ^{13}C and ^{1}H isotropic chemical shifts (with respect to TMS all values in ppm) for NNT2CAH.

Atom	Experimental	DFT/B3LYP		
		6-31G(d)	6-31G(d, p)	6–311G(d, p)
C1	167.29	148.91	153.56	166.81
C2	111.31	98.59	102	119.73
C3	155.30	145.29	150.04	159.9
C4	30.71	16.4	19.66	36.01
C5	41.04	25.15	27.75	46.19
C6	38.75	29.82	34.06	45.58
C7	41.04	22.7	25.27	46.2
C8	30.06	7.32	9.44	34.51
C9	152.26	142.95	147.98	164.4
C10	124.70	108.88	112.22	131.86
C11	127.69	111.78	115.36	134.93
C12	125.34	106.89	110.43	131.51
C13	127.69	110.8	114.38	134.94
C14	124.70	109.06	112.49	131.86
C15	146.02	134.19	137.44	150.22
C16	138.49	129.54	134.61	151.11
C17	128.27	121.74	125.27	140.66
C18	132.17	113.72	117.39	133.25
C19	129.47	118.8	122.32	141.64
C20	43.66	37.08	40.22	56.75
C21	156.27	156.8	161.3	174.25
H2	6.85	2.92	4	6.93
H4	3.79	0.26	0.94	3.7
H5*	2.68	0.82	0.16	2.71
H7*	2.52	0.85	0.255	2.71
H8*	1.60	3.21	2.61	1.54
H10	6.87	4.47	5.41	7.54
H11	6.98	4.64	5.57	7.74
H12	6.96	4.65	5.58	7.68
H13	7.05	4.87	5.81	7.74
H14	7.03	4.58	5.53	7.55
H15	9.40	6.96	8.14	10.95
H17	7.17	2.52	3.51	5.89
H18	7.20	3.86	4.84	7
H19	7.24	4.21	5.24	7.64
H20*	4.82	1.34	2.09	4.98

***: Average.*

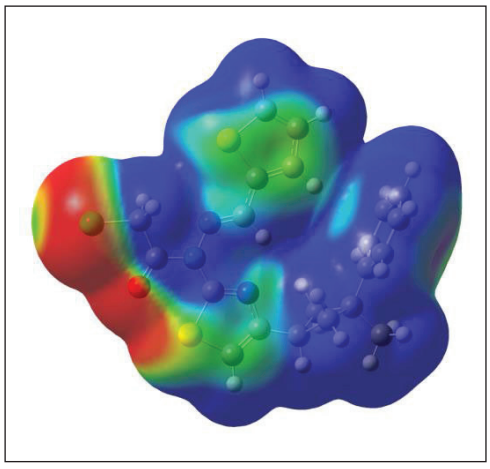

Figure 4. Molecular electrostatic potential map calculated at B3LYP/6-311G(d,p) level.

regions are mainly over the Cl and O atoms. The negative V(r) values are -0.0530 a.u. for O atom, which is the most negative region: About -0.0272 a.u. for Cl atom and -0.0217 a.u. for S atom, which is the least negative region. As we have mentioned earlier, the electrostatic potential has been used primarily for predicting sites and relative reactivities towards electrophilic attack, and in studies of biological recognition and hydrogen bonding interactions (Munoz-Caro et al. 2000).

3.6. HOMO–LUMO Analysis

The highest occupied molecular orbital (HOMO) and lowest unoccupied molecular orbital (LUMO) are the main

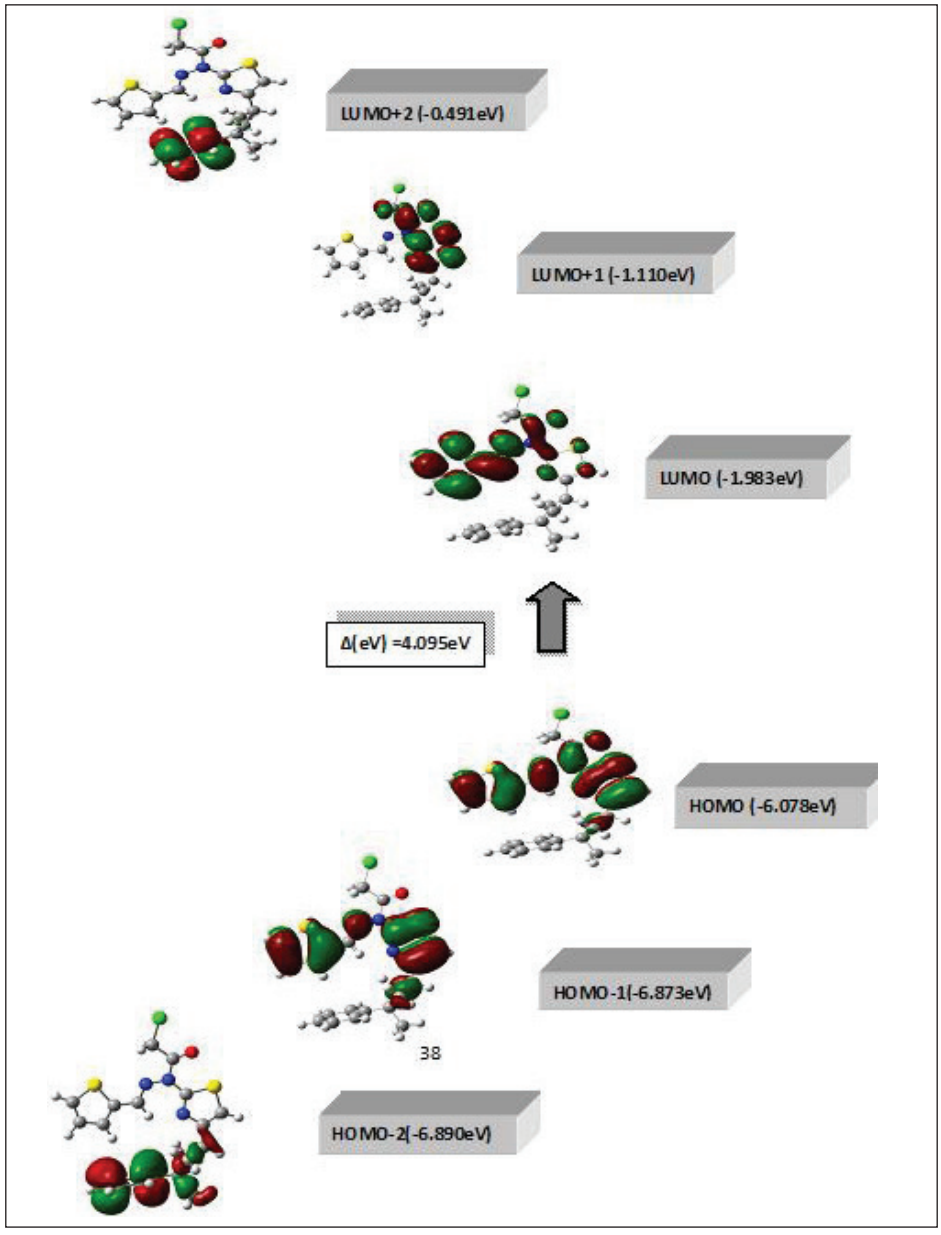

Figure 5. The atomic orbital composition of the frontier molecular orbital for NNT2CAH.

orbital and take part in chemical stability (Gunasekaran et al. 2008). The HOMO represents the ability to donate an electron, while LUMO as an electron acceptor represents the ability to obtain an electron. This electronic transition absorption corresponds to the transition from the ground to the first excited state and is mainly described by an electron excitation from the highest occupied molecular orbital (HOMO) to the lowest unoccupied molecular orbital (LUMO). Owing to the interaction between HOMO and LUMO orbital of a structure, the transition state of $\pi-\pi^*$ type is observed with regard to the molecular orbital theory (Fukui 1975, Fukui 1982). Therefore, while the energy of the HOMO is directly related to the ionization potential, LUMO energy is directly related to the electron affinity. The energy difference between HOMO and LUMO orbital is called as energy gap that is an important stability for structures (Lewis et al. 1994). The value of the energy separation between the HOMO and LUMO is 4.095 eV for B3LYP/6-311G(d,p) level and this gap demonstrates that the title compound is stable (Demir et al. 2012). In addition, 3D plots of frontier molecular orbitals and energy values are shown in Figure 5.

4. Conclusion

In this work, we calculated the geometrical parameters and vibrational frequencies and some molecular properties of the monomer form of the *N*-[4-(3-methyl-3-phenyl-cyclobutyl)-thiazol-2-yl]-*N'*-thiophen-2ylmethylene-Chloro-acetic acid hydrazide molecule by using B3LYP method for 6-31G(d), 6-31G(d,p) and 6-311G(d,p) basis sets. To support the solid state structure, the geometric parameters, vibrational frequencies and ^{1}H and ^{13}C NMR chemical shifts were theoretically determined through comparision with experimental data. A good correlation between the experimental and computed values was observed. The conformational stability was determined to find the most stable form of the title compound.

5. References

Andersson, MP., Uvdal, P. 2005. New Scale Factors for Harmonic Vibrational Frequencies Using the B3LYP Density Functional Method with the Triple-ζ Basis Set 6-311+G(d,p). *J. Phys. Chem. A*, 109, 2937-2941.

Coates, J. 2000. Interpretation of Infrared Spectra, A Practical Approach. In Encyclopedia of Analytical Chemistry, Meyers, R.A., Ed., John Wiley & Sons, Ltd: Chichester, UK, pp. 10815-10837.

Demir, S., Dincer, M., Cukurovali, A., Yilmaz, I. 2012. Experimental and Theoretical Investigation of the Molecular and Electronic Structure of N´-Benzylidene-N-[4-(3-methyl-3-phenyl-cyclobutyl)-thiazol-2-yl]-chloro-acetic acid hydrazide. *Int. J. Quantum Chem.* 112, 2: 1016-1028.

Frisch, MJ., Trucks, GW., Schlegel, HB., Scuseria, G. E., Robb, MA., Cheeseman, J. R., Scalmani, G., Barone, V., Mennucci, B., Petersson, GA., Nakatsuji, H., Caricato, M., Li, X., Hratchian, HP., Izmaylov, AF., Bloino, J., Zheng, G., Sonnenberg, JL., Hada, M., Ehara, M., Toyota, K., Fukuda, R., Hasegawa, J., Ishida, M., Nakajima, T., Honda, Y., Kitao, O., Nakai, H., Vreven, T., Montgomery, JAJr., Peralta, JE., Ogliaro, F., Bearpark, M., Heyd, JJ., Brothers, E., Kudin, KN., Staroverov, VN., Kobayashi, R., Normand, J., Raghavachari, K., Rendell, A., Burant, JC., Iyengar, S. S., Tomasi, J., Cossi, M., Rega, N., Millam, JM., Klene, M., Knox, JE., Cross, JB., Bakken, V., Adamo, C., Jaramillo, J., Gomperts, R., Stratmann, RE., Yazyev, O., Austin, AJ., Cammi, R., Pomelli, C., Ochterski, JW., Martin, RL., Morokuma, K., Zakrzewski, VG., Voth, GA., Salvador, P., Dannenberg, JJ., Dapprich, S., Daniels, AD., Farkas, Ö., Foresman, JB., Ortiz, JV., Cioslowski, J., Fox, DJ. 2004. Gaussian 03, Revision E.01, Gaussian, Inc., Wallingford CT.

Foresman, JB., Frisch, A. 1996. Exploring Chemistry with Electronic Structure Methods, second ed., Gaussian Inc., Pittsburgh, PA.

Fukui, K. 1975. Theory of Orientation and Stereo Selection, Springer-Verlag, New York.

Gunasekaran, S., Balaji, RA., Kumerasan, S., Anand, G., Srinivasan, S. 2008. Experimental and theoretical investigations of spectroscopic properties of N-acetyl-5-methoxytryptamine. *Can. J. Anal. Sci. Spectrosc.* 53: 149-160.

Hehre, WJ., Ditchfield, R., Pople, JA. 1972. Self—consistent molecular orbital methods. XII. Further extensions of gaussian—type basis sets for use in molecular orbital studies of organic molecules. J. Chem. Phys. 56(5): 2257-2261.

Jaen, JC., Wise, L.D., Caprathe, B.W., Tecle, H., Bergmeier, H., Humblet, CC., Heffner, TG., Meltzner, LT., Pugsley, TA. 1990. 4-(1,2,5,6-Tetrahydro-1-alkyl-3-pyridinyl)-2-thiazolamines: a novel class of compounds with central dopamine agonist properties. J. *Med. Chem.*, 33: 311-7.

Karakurt, T., Dincer, M., Cukurovali A., Yilmaz, I. 2011. Ab initio and semi-empirical computational studies on 5-hydroxy-4-methyl-5, 6-di-pyridin-2-yl-4, 5-dihydro-2H-[1, 2, 4] triazine-3-thione. *J. Mol. Struct.,* 991:186-201.

Khalil, AM., Berghot, MA., Gouda, MA. 2009. Synthesis and antibacterial activity of some new heterocycles incorporating phthalazine. *Eur. J. Med. Chem.*, 44 (11): 4434-4440.

Koike, K., Jia Z., Nikaido, T., Liu, Y., Zhao, Y., Guo, D. 1999. Echinothiophene, a Novel Benzothiophene Glycoside from the Roots of Echinops grijissii. *Org. Lett.,* 1: 197-198.

Metzger, JV. 1979. Thiazole and Its Derivatives, 1st ed.; John Wiley and Sons: New York, NY, USA, p 612.

Munoz-Caro, C., Ni¯no, A., Senent, ML., Leal, JM., Ibeas, S. 2000. Modeling of protonation processes in acetohydroxamic acid. *J. Org. Chem.,* 65: 405-410.

Panicker, CY., Varghese, HT., Philip, D., Nogueira, HIS., Kastkova, K. 2007. Raman, IR and SERS spectra of methyl(2-methyl-4,6-dinitrophenylsulfanyl)ethanoate. *Spectrochim. Acta A,* 67: 1313-1320.

Patt, WC., Hamilton, HW., Taylor, MD., Ryan, MJ., Taylor, Jr. DG., Connolly, CJC., Doherty, AM., Klutchko, SR., Sircar, I., Steinbaugh, BA., Batley, BL., Painchaud, CA., Rapundalo, ST., Michniewicz, BM., Olson, SCJ. 1992. Structure-activity relationships of a series of 2-amino-4-thiazole-containing renin inhibitors. *J. Med. Chem.*, 35: 2562-2572.

Pavia, DI., Lampman, GM., Kriz, GS. 2001. Physics in: J. Vondeling (Ed.), Introduction to Spectroscopy: A Guide for Student of Organic Chemistry, third ed., Thomson Learning, p 579.

Politzer, P. 1981. Truhlar (Eds), D.G. Chemical Applications of Atomic and Molecular Electrostatic Potentials. Plenum Press, New York.

Pozharskii, AF., Soldatenkov, AT., Katritzky, AR. 1997. Heterocycles in life and society, 1st. ed., 301 p., John Wiley & Sons.

Schlegel, HB. 1982. Optimization of equilibrium geometries and transition structures. J. Comp. Chem., 3(2): 214-218.

Sharma, PK., Sawnhney, SN., Gupta, A., Singh, GB., Bani, S. 1998. Synthesis and antiinflammatory activity of some 3-(2-thiazolyl)-1,2-benzisothiazoles. *Indian J. Chem.* 37B: 376-381.

Sheldrick, GM. 1997. SHELXS-97 and SHELXL-97, Program for Crystal Structure Determination; University of Göttingen: Germany.

Sıdır, I., Sıdır, YG., Tasal, E., Ogretir, C. 2010. density functional theory inestigations on the conformational stability, molecular structure and vibrational spectra of 3-(2-(4-methylpiperazin-1-yl)-2-oxeoethyl) benzo [d] thiazol-2 (3H)-one. *J. Mol. Struct.,* 980: 230-244.

Silverstein, M. 2003. Webster FX: Spectrometric Identification of Organic Compounds. Sixth ed., John Wiley, Asia.

Stuart, B. 2008. Infrared Spectroscopy: Fundamentals and Applications. John Wiley and Sons, Ltd.

Tsuji, K., Ishikawa, H. 1994. Synthesis and anti-pseudomonal activity of new 2-isocephems with a dihydroxypyridone moiety at C-7. *Bioorg. Med. Chem. Lett.,* 4: 1601-1606.

Walczynski, K., Guryn, R., Zuiderveld, OP., Timmermann, H. 1999. Non-imidazole histamine H3 ligands. Part I. Synthesis of 2-(1-piperazinyl)- and 2-(hexahydro-1H-1,4-diazepin-1-yl)benzothiazole derivatives as H3-antagonists with H1 blocking activities. *Farmaco,* 54: 684-694.

Wipf, P., Wang, Z. 2007. Total synthesis of N^{14}-desacetoxytubulysin *H. Org. Lett.,* 98: 1605–1607.

Wolinski, K., Hilton, JF., Pulay, P. 1990. Efficient implementation of the gauge-independent atomic orbital method for NMR chemical shift calculations. *J. Am. Chem. Soc.,* 112: 8251-8260.

Yadav, RA., Sing, IS. 1985. Intermolecular hydrogen-bonding in o-ethyl and m-ethyl phenols. *Indian J. Pure Appl. Phys.,* 23: 626-627.